Published OnlineFirst September 17, 2013; DOI: 10.1158/1078-0432.CCR-13-0526

Clinical Cancer Research

Hypoxic Activation of the PERK/eIF2α Arm of the Unfolded Protein Response Promotes Metastasis through Induction of LAMP3

Hilda Mujcic, Anika Nagelkerke, Kasper M.A. Rouschop, et al.

Clin Cancer Res 2013;19:6126-6137. Published OnlineFirst September 17, 2013.

Published OnlineFirst September 17, 2013; DOI: 10.1158/1078-0432.CCR-13-0526

Human Cancer Biology

Clinical Cancer Research

Hypoxic Activation of the PERK/eIF2α Arm of the Unfolded Protein Response Promotes Metastasis through Induction of LAMP3

Hilda Mujcic[1,8], Anika Nagelkerke[9], Kasper M.A. Rouschop[8], Stephen Chung[1], Naz Chaudary[1], Paul N. Span[9], Blaise Clarke[2], Michael Milosevic[3,5], Jenna Sykes[6], Richard P. Hill[1,3,4], Marianne Koritzinsky[1,2,3,7], and Bradly G. Wouters[1,2,3,4]

Abstract

Purpose: Conditions of poor oxygenation (hypoxia) are present in many human tumors, including cervix cancer, and are associated with increased risk of metastasis and poor prognosis. Hypoxia is a potent activator of the PERK/eIF2α signaling pathway, a component of the unfolded protein response (UPR) and an important mediator of hypoxia tolerance and tumor growth. Here, the importance of this pathway in the metastasis of human cervix carcinoma was investigated.

Experimental Design: Amplification and expression of *LAMP3*, a UPR metastasis-associated gene, was examined using FISH and immunofluorescence in a cohort of human cervix tumors from patients who had received oxygen needle electrode tumor oxygenation measurements. To evaluate the importance of this pathway in metastasis *in vivo*, we constructed a series of inducible cell lines to interfere with PERK signaling during hypoxia and used these in an orthotopic cervix cancer model of hypoxia-driven metastasis.

Results: We show that LAMP3 expression in human cervix tumors is augmented both by gene copy number alterations and by hypoxia. Induced disruption of PERK signaling in established orthotopic xenografts resulted in complete inhibition of hypoxia-induced metastasis to the lymph nodes. This is due, in part, to a direct influence of the UPR pathway on hypoxia tolerance. However, we also find that LAMP3 is a key mediator of hypoxia-driven nodal metastasis, through its ability to promote metastatic properties including cell migration.

Conclusion: These data suggest that the association between hypoxia, metastasis, and poor prognosis is due, in part, to hypoxic activation of the UPR and expression of LAMP3. *Clin Cancer Res; 19(22); 6126–37. ©2013 AACR.*

Introduction

The microenvironment of solid tumors is profoundly different from that of the normal tissues from which they derive. Tumor proliferation coupled with insufficient vasculature results in poorly oxygenated (hypoxic) regions where oxygen and nutrient demand exceeds supply. Clinical studies have established an association between tumor hypoxia and poor patient prognosis in several tumor types. For example, large clinical studies have shown that the hypoxic fraction measured by oxygen electrodes is prognostic in uterine cervix and head and neck carcinoma (1–3). Tumor hypoxia negatively impacts prognosis by conferring resistance to both radio- and chemotherapy and also induces biologic changes that promote increased malignancy, including metastasis (4–6). Studies in both cervix carcinoma and soft tissue sarcoma have shown that patients with hypoxic tumors are more likely to fail therapy due to distant metastases (4, 5, 7). Likewise, a recent study in prostate cancer has identified tumor hypoxia as an independent predictor of biochemical relapse, but only within the first 48 months of completing treatment, suggesting the presence of subclinical metastatic disease at time of treatment in patients with hypoxic tumors (8). Laboratory and animal models support a direct role for hypoxia in promoting metastasis. *In vitro* hypoxia exposure has been shown to

Authors' Affiliations: [1]Ontario Cancer Institute and Campbell Family Institute for Cancer Research, Princess Margaret Cancer Centre, University Health Network; Departments of [2]Laboratory Medicine and Pathobiology, [3]Radiation Oncology, and [4]Medical Biophysics; [5]Radiation Medicine Program, [6]Department of Biostatistics, Princess Margaret Cancer Centre, [7]Institute of Medical Science, University of Toronto, Toronto, Ontario, Canada; [8]Maastricht Radiation Oncology (MaastRO) Lab, GROW – School for Oncology and Developmental Biology, Maastricht University, Maastricht; and [9]Departments of Radiation Oncology and Laboratory Medicine, Radboud University Nijmegen Medical Centre, Nijmegen, the Netherlands

Note: Supplementary data for this article are available at Clinical Cancer Research Online (http://clincancerres.aacrjournals.org/).

Corresponding Author: Bradly G. Wouters, 610 University Ave, Toronto, ON, M5G 2M9, Canada. Phone: 1-416-581-7840; Fax: 1-416-946.2984; E-mail: bwouters@uhnresearch.ca

doi: 10.1158/1078-0432.CCR-13-0526

Published OnlineFirst September 17, 2013; DOI: 10.1158/1078-0432.CCR-13-0526

Translational Relevance

Tumor hypoxia promotes both treatment resistance and metastasis. Large well-controlled clinical studies have shown a clear association between primary tumor hypoxia and distant metastasis that influences overall survival. Here, we report that the unfolded protein response (UPR), a prosurvival pathway that is activated during hypoxia, is also an important mediator of metastasis in human cervix cancer. We found that the UPR target gene LAMP3, a putative metastasis-promoting gene, is regulated by hypoxia in primary human cervix cancer biopsies obtained from trials where hypoxia was measured using oxygen needle electrodes. Furthermore, we developed isogenic, orthotopic cervical models and could show a direct role for UPR signaling and specifically LAMP3 in promoting hypoxia-induced metastasis to the lymph nodes. Collectively, our findings show that hypoxic activation of the UPR is a driver of metastasis and a contributor to the poor prognosis of patients with cervical cancer.

potentiate experimental metastasis of several cancer cell lines when injected into mice (9–12). Moreover, increasing tumor hypoxia by subjecting tumor-bearing animals to periodically breathe low-oxygen gas increases metastasis in a number of models, including an orthotopic model of human cervical carcinoma (13–15).

Tumor cells respond to hypoxia through several adaptive oxygen-sensitive signaling pathways. This includes activation of the hypoxia-inducible factor family of transcription factors (HIF), which regulate the expression of many genes involved in metabolism and angiogenesis (16). Hypoxia also acts as a potent activator of the unfolded protein response (UPR), an evolutionally conserved program that responds to endoplasmic reticulum (ER) stress (17–19). The UPR consists of 3 signaling pathways initiated by PKR-like ER kinase (PERK, also known as EIF2AK3), inositol-requiring enzyme 1 (IRE1), and activating transcription factor 6 (ATF6). Several studies have shown that both PERK and IRE1 arms of the UPR are strongly activated by hypoxia and important for the tolerance of tumor cells to hypoxic stress (19–22). PERK activation leads to a rapid inhibition of protein synthesis during hypoxia through phosphorylation of the α subunit of eukaryotic translation initiation factor 2 (eIF2α) on Ser51 (18). Paradoxically, eIF2α phosphorylation also results in selective translation of activating transcription factor 4 (ATF4) due to the presence of an unusual 5′-untranslated region (UTR) that contains multiple upstream open reading frames (17, 23, 24). ATF4 initiates a widespread transcriptional response that mediates adaptation to ER stress (25). ATF4 promotes hypoxia tolerance directly by inducing LC3B (MAP1LC3B) that enables high rates of autophagy required to protect hypoxic cells from cell death (26). Finally, ATF4 also initiates a negative feedback loop by inducing growth arrest and DNA damage-inducible protein 34 (GADD34, also known as PPP1R15A), which promotes dephosphorylation of eIF2α and restoration of protein synthesis (27).

Several studies have shown that HIF1 activation can regulate pathways involved in metastasis (28, 29). Direct or indirect targets of HIF1 include genes that regulate the epithelial and mesenchymal transition (EMT), matrix metalloproteinases (MMP), and lysyl oxidase (LOX), which is involved in the establishment of the premetastatic niche (30–32). The relevance of UPR signaling in hypoxia-induced metastasis has not been examined. However, we recently showed that expression of a putative metastasis-promoting gene, lysosomal-associated membrane protein 3 (LAMP3) is strongly induced by hypoxia in a PERK/ATF4-dependent and HIF-independent manner (33). LAMP3 has been hypothesized as a potential mediator of metastasis and is overexpressed in several cancer types (34). Here, we examined the expression and hypoxic regulation of LAMP3 in primary human cervix tumors with known oxygenation status. We have also created a series of isogenic and inducible cell models and used these in an orthotopic model of cervical cancer to test the contribution of PERK and LAMP3 in hypoxia-induced metastasis *in vivo*.

Materials and Methods

Cell models and hypoxia exposure

The ME180 (human cervix carcinoma; normal LAMP3 gene copy number) cell line with doxycycline-inducible expression of the hamster GADD34 C-terminus (GADD34-C) (35) was created using the Flp-In T-Rex system according to the manufacturer's instructions (Invitrogen). ME180 cells (a kind gift from Dr. Richard Hill, Princess Margaret Cancer Centre, Toronto, ON, Canada) were transfected with a pRetroSuper vector containing a short hairpin against LAMP3 to generate stable LAMP3 knockdown cells (shLAMP3) or with an empty vector (EV control). All cell lines have been authenticated using short tandem repeat (STR) profiling conducted by The Centre for Applied Genomics, The Hospital for Sick Children, Toronto, Canada. For anoxic exposure, cells were transferred into a H85 HypOxystation hypoxic incubator (Hypoxgyen). The composition of the atmosphere in the incubator consisted of 5% H_2, 5% CO_2, 0.0% O_2, and residual N_2.

RNA isolation and quantitative PCR analysis

Total RNA isolation and quantitative real-time PCR were carried out as previously described (33). Relative transcript abundance was determined using the standard curve method and normalized to 18S rRNA expression.

Western blot analysis

Cell lysis and immunoblot analysis was conducted as described previously (33). For the detection of phosphorylated eIF2α, cells were lysed in 20 mmol/L HEPES, 100 mmol/L KCl, 5 mmol/L EDTA, 10% glycerol, 0.5% Triton-X, 0.005% SDS, and 1 mmol/L dithiothreitol (DTT) supplemented with Halt Phosphatase Inhibitor Cocktail

Published OnlineFirst September 17, 2013; DOI: 10.1158/1078-0432.CCR-13-0526

(Thermo Scientific). See Supplementary Materials and Methods for antibodies used.

Spontaneous metastasis assay and cyclic hypoxia treatment

Orthotopic implantations were conducted as described previously (13). Expression of the GADD34-C transgene was induced 8 days after implantation by administration of doxycycline (2 g/L in 5% sucrose) in the drinking water of the animals. The cyclic hypoxia treatment was started the following day (day 9) and consisted of alternating exposure to 10 minutes of 7% oxygen and 10 minutes of standard laboratory air for a total of 4 hours a day, 7 days a week until 24 hours before sacrifice, as described previously (13, 36). Upon sacrifice, the primary cervix tumors were removed and colonized lymph nodes of the pelvic nodal chain, which at this point are visible to the naked eye, were counted. The chain consists of a total of 8 nodes, aligned in 4 pairs. Metastatic efficiency was expressed as the total number of colonized lymph nodes per animal, or as metastatic score, which was calculated using the formula: $(p_1 \times 1) + (p_2 \times 1) + (p_3 \times 2) + (p_4 \times 3)$ where p_1 is the number of involved nodes for lymph node pair 1, p_2 is the number of involved nodes for lymph node pair 2, etc. Pair one and pair two were given an equal weight because they are located at a similar distance from the primary tumor and colonization of pair one has been shown to be independent of hypoxia exposure (13). To identify viable hypoxic cells, animals were injected with the hypoxia marker drug EF5 [2-(2-nitro-1*H*-imidazole-1-yl)-*N*-(2,2,3,3,3-pentafluoropropyl) acetamide], obtained from Dr. Cameron Koch (University of Pennsylvania), 4 hours before tumor excision (100 μmol/kg intraperitoneally). All animal experiments were carried out according to the regulations of the Canadian Council on Animal Care.

Immunohistochemical staining and image analysis

See Supplementary Materials and Methods for the staining protocols. Images were analyzed using Definiens Tissue Studio software, which allows for semi-automatic histology image analysis. Briefly, the software was trained to identify viable tumor areas, necrotic areas, tumor stroma, and empty areas within the scanned section. For primary human cervix carcinoma biopsies, the average LAMP3 staining intensity within the tumor areas was measured as well as the LAMP3-positive area above a background threshold obtained from the average intensity of all patient sections. The product of average staining intensity and fractional labeled tumor area was calculated for each case to represent relative protein abundance. Two sections per case were stained and analyzed at different times.

FISH analysis

The LAMP3-containing clone RP11-1012H23 was selected from the Human UCSC Genome Browser assembly (Feb.2009 CRch37/hg19) and obtained from TCAG Genome Resource Facility (Toronto, ON, Canada). Before experiments, the RP11-1012H23 probe was verified on normal blood metaphases to confirm its correct location on chromosome 3q27. The BAC probe was used along with centromeric probes CEP3 (labeled with SpG) and CEP7 (labeled with aqua) purchased from Abbott Molecular and used as internal controls. FISH was conducted on paraffin-embedded tissue microarrays (TMA). See Supplementary Materials and Methods for protocol. Hematoxylin and eosin (H&E)-stained adjacent TMA sections were compared with FISH stained slides to properly identify tumor cells. Hundred nonoverlapping, intact cells were scored for each case. Total LAMP3, CEP3, and CEP7 signal was determined for each case and subsequently the LAMP3 to CEP3 and LAMP3 to CEP7 ratio was calculated. A ratio of 1.5 or higher was considered an abnormal signal.

Patients and oxygen measurements

Biopsies were obtained from a previously described group of patients with uterine cervix cancer enrolled in a single institutional prospective study (37). Written informed consent was obtained from each participant before study entry and the Research Ethics Board at the Princess Margaret Cancer Centre approved the trial. The clinical characteristics of the group of patients with LAMP3 protein expression (IHC) are found in Supplementary Table S1. The first date of treatment in this group was January 25, 2000 and the last April 25, 2007. The median follow-up is 5.9 years (range, 0.8–10.6).

Statistical analysis

Unless stated otherwise, the 2-sample Student *t* test or one-way ANOVA with Bonferroni's *post hoc* test were used to test for differences in numerical data. Correlations between 2 continuous variables were measured using Spearman's correlation. Linear regressions were used to assess the associations between LAMP3 expression and clinical variables (nodal status, FIGO stage, and grade). Analyses were done using R version 2.12.1 and GraphPad Prism 5. Two-sided *P* values of less than 0.05 were considered statistically significant.

Results

LAMP3 expression correlates with hypoxia in primary human cervix tumors

We recently showed that LAMP3, a protein implicated in cervical cancer metastasis, is induced by hypoxia through activation of the PERK/eIF2α/ATF4-dependent arm of the UPR (33). To evaluate the clinical relevance of these findings, we investigated whether hypoxia also influences LAMP3 expression in patients with cervical cancer, a disease in which hypoxia is associated with increased metastasis and poor overall survival (5, 7). LAMP3 was examined in a cohort of cervical carcinoma patient samples obtained from clinical trials at the Princess Margaret Cancer Centre in which patient tumors had been previously assessed for hypoxia with oxygen needle electrodes before treatment. LAMP3 expression was assessed in the same patients at both the mRNA and protein levels. As copy number gains and amplifications of LAMP3 have been reported in cervix

Published OnlineFirst September 17, 2013; DOI: 10.1158/1078-0432.CCR-13-0526

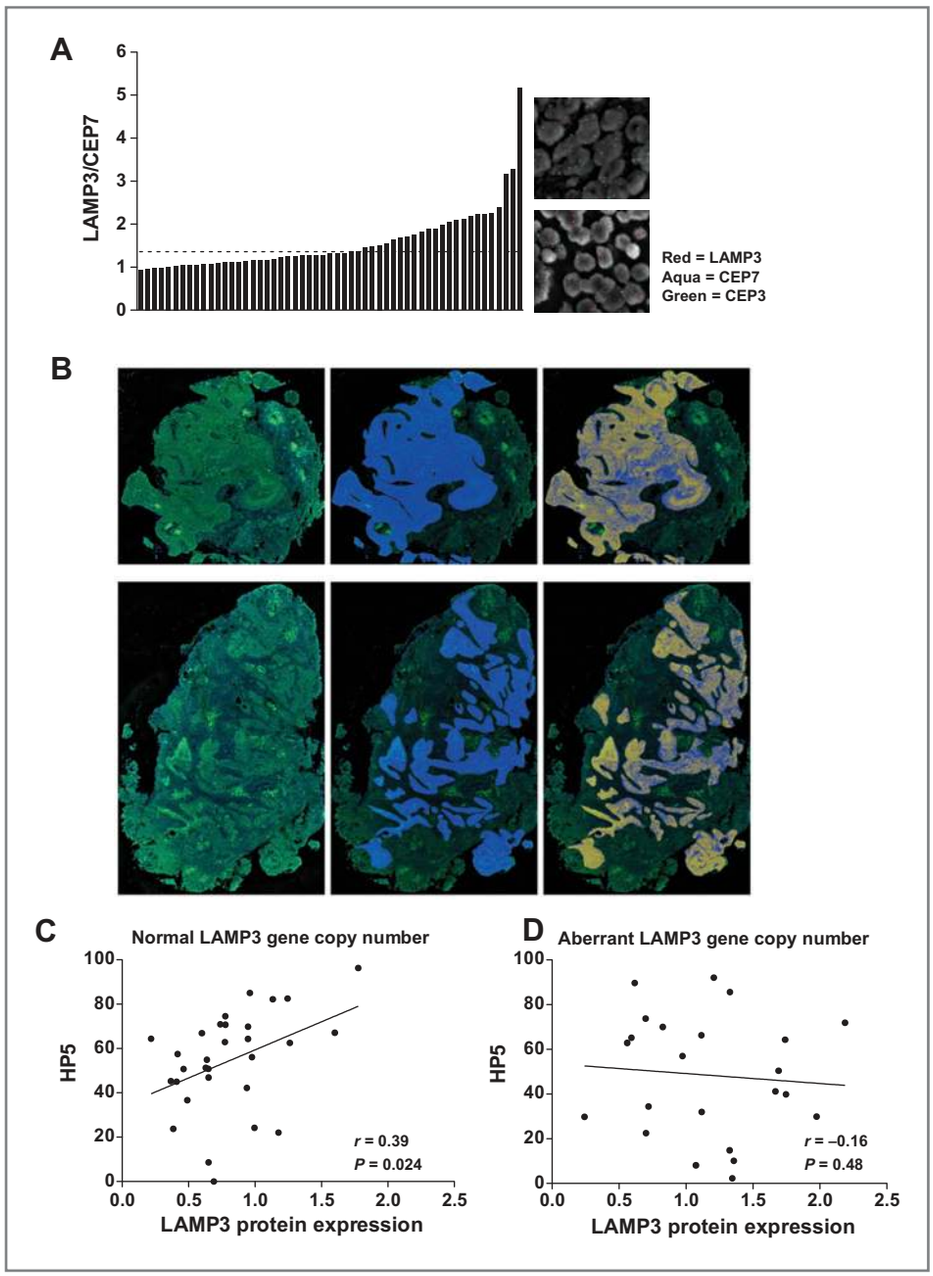

Figure 1. LAMP3 expression correlates with the degree of hypoxia in primary human cervix tumors. A, left, waterfall plot of LAMP3/CEP7 ratios measured in human cervical cancer biopsies, $n = 55$. Dashed line represents the cutoff between normal and aberrant LAMP3 gene copy numbers. Right, representative images of cases with normal (top) and amplified (bottom) LAMP3 copy numbers. LAMP3, red signal; CEP7, aqua; CEP3, green. B, LAMP3 protein expression quantification exemplified in 2 human cervix tumors. Top and bottom left, immunofluorescence staining of total biopsy sections for LAMP3 (green, unthresholded signal), overlaid with 4′,6-diamidino-2-phenylindole (DAPI) signal (blue); top and bottom middle, viable tumor areas within sections indicated in blue; top and bottom right, LAMP3 (thresholded signal) within viable tumor areas. Scatter plots of HP5 values and LAMP3 expression in patients with (C) normal (LAMP3/CEP7 < 1.5, $n = 34$) and (D) aberrant (LAMP3/CEP7 ≥ 1.5, $n = 21$) LAMP3 gene copy numbers. A straight line was fitted through the data. (Spearman correlation test.)

cancer (38), we also assessed LAMP3 copy number aberrations using FISH. Consistent with previously reported results, genomic gains or amplifications in LAMP3 were observed in 38% of all cases examined (Fig. 1A). A weak but significant relationship was also observed between LAMP3 copy number (as estimated by FISH) and both LAMP3 mRNA and protein expression (Supplementary Fig. S1A and S1B, respectively). No LAMP3 copy number aberrations were identified in normal cervix tissue (Supplementary Fig. S1C).

Using quantitative immunofluorescence, LAMP3 protein expression was measured specifically within the viable epithelial tumor areas (excluding stroma) of all patient biopsies as depicted in Fig. 1B. Tumor-infiltrating, LAMP3-positive, mature dendritic cells were also excluded from the analysis. As reported earlier (33), LAMP3 staining intensity was highly heterogeneous and the protein was found primarily on the plasma membrane. To examine the influence of hypoxia on LAMP3 expression, we separated patients into groups with normal LAMP3 copy number and those with gains or amplifications. Importantly, in patients with normal LAMP3 copy numbers, a positive and significant association between hypoxia (HP5) and LAMP3 expression was observed (Fig. 1C and D and Supplementary

Published OnlineFirst September 17, 2013; DOI: 10.1158/1078-0432.CCR-13-0526

Table S2), whereas no such correlation was seen in the subset with copy number gains or amplifications in LAMP3. These data indicate that LAMP3 expression in cervical cancer is influenced through both genetic means (copy number gains and amplifications) and hypoxia. A subgroup analysis showed a positive relationship between LAMP3 expression and clinical stage at diagnosis, but again only in patients with normal copy numbers (Supplementary Table S3), indicating that LAMP3 may be one of the mechanisms through which hypoxia promotes more aggressive disease.

Generation of an isogenic inducible PERK signaling defective cervical cancer xenograft model

To address the functional importance of UPR and LAMP3 activation in hypoxia-induced metastasis, we focused first on the requirement for the PERK signaling arm. We selected the ME180 cervical carcinoma cell line that when grown orthotopically in the mouse cervix metastasizes to the lymph nodes in a hypoxia-regulated manner (13, 39). We introduced a flippase recombination target site together with a tetracycline repressor into this line and tested its functionality by inserting a doxycycline-regulated eGFP reporter into the target site. Doxycycline resulted in strong induction of eGFP expression both *in vitro* and *in vivo* (Supplementary Fig. S2 and Fig. 2A, respectively). Importantly, the potential of the ME180 cell line to spread to the local pelvic lymph nodes when grown orthotopically was maintained (Supplementary Fig. S3A–S3C) and doxycycline treatment alone had no effect on lymph node metastasis (Supplementary Fig. S3D–S3F).

Next, we generated an ME180 subline with doxycycline-regulated expression of the C-terminal region of the hamster GADD34 protein (referred to as ME180-GADD34-C). Overexpression of this protein promotes dephosphorylation of eIF2α and thus prevents signaling through the PERK arm of the UPR (35). Maximum induction of GADD34-C is

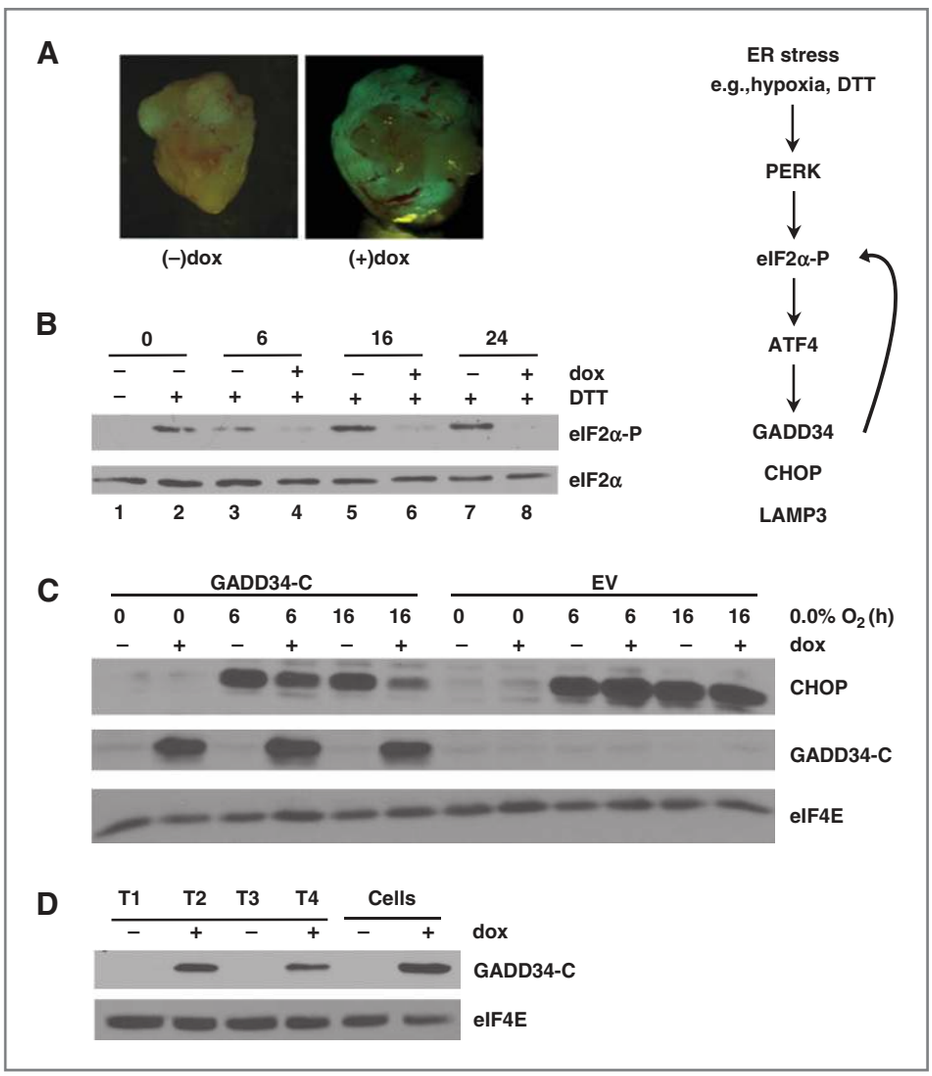

Figure 2. A doxycycline-regulated ME180 cervix carcinoma cell line with inducible expression of the GADD34 protein. A, EGFP expression in orthotopic xenografts established from cells. Doxycycline was administered to tumor-bearing mice in water (2 g/L) for a total period of 2 weeks. EGFP expression was evaluated under a fluorescent stereomicroscope. B, right, the PERK/eIF2α/ATF4 arm of the UPR. Left, DTT-induced phosphorylation of eIF2α was assessed by immunoblotting in ME180-GADD34-C cells pre-exposed to 0, 6, 16, or 24 hours of doxycycline. Total eIF2α protein levels were used as loading control. C, ME180-GADD34-C and EV control cells were preincubated with doxycycline for 72 hours (+dox) or left untreated (−dox), and subsequently exposed to 0, 6, or 16 hours of anoxia. CHOP protein expression was measured by immunoblotting. D, GADD34 transgene protein expression was assessed in 4 different intramuscularly grown ME180-GADD34-C derived xenografts (T1–T4) following a 7-day administration of doxycycline to the animals.

Published OnlineFirst September 17, 2013; DOI: 10.1158/1078-0432.CCR-13-0526

reached after 8 hours of doxycycline treatment and persists for 48 hours (Supplementary Fig. S4A). To test the functionality of these cells, we exposed them to the potent ER stress–inducing agent DTT. DTT induced strong phosphorylation of eIF2α in the ME180-GADD34-C cells (Fig. 2B, lanes 2, 3, 5, 7), which was prevented in cells exposed to doxycycline for 6, 16, or 24 hours (Fig. 2B, lanes 4, 6, 8). Functionality was then tested in cells exposed to severe hypoxia (<0.02% O_2) by monitoring downstream activation of the UPR target gene CHOP. In doxycycline-free cells, hypoxia caused a rapid induction of both CHOP protein (Fig. 2C) and mRNA (Supplementary Fig. S4B), which again was strongly inhibited in cells exposed to doxycycline. Importantly, inducible expression of GADD34 was also detectable in tumor xenografts at levels comparable to those *in vitro* (Fig. 2D).

Disruption of UPR signaling inhibits hypoxia-induced lymph node metastasis

The metastatic potential of ME180 cells with intact versus defective PERK signaling was tested by implanting ME180-GADD34-C xenografts orthotopically and allowing them to establish for eight days before expressing the GADD34 transgene with doxycycline. This approach eliminates confounding effects of the transgene on primary tumor establishment, which is influenced by PERK (20). Starting on day 9, tumor-bearing mice were exposed daily to a cycling hypoxia regimen that promotes lymph node metastasis in this model (ref. 13; Fig. 3A). As observed previously, doxycycline-free tumors (with a functional PERK pathway) from hypoxia-treated animals were noticeably smaller than sham-treated mice (Fig. 3B; compare −dox sham and −dox hypoxia; refs. 13, 36). Doxycycline-induced disruption of

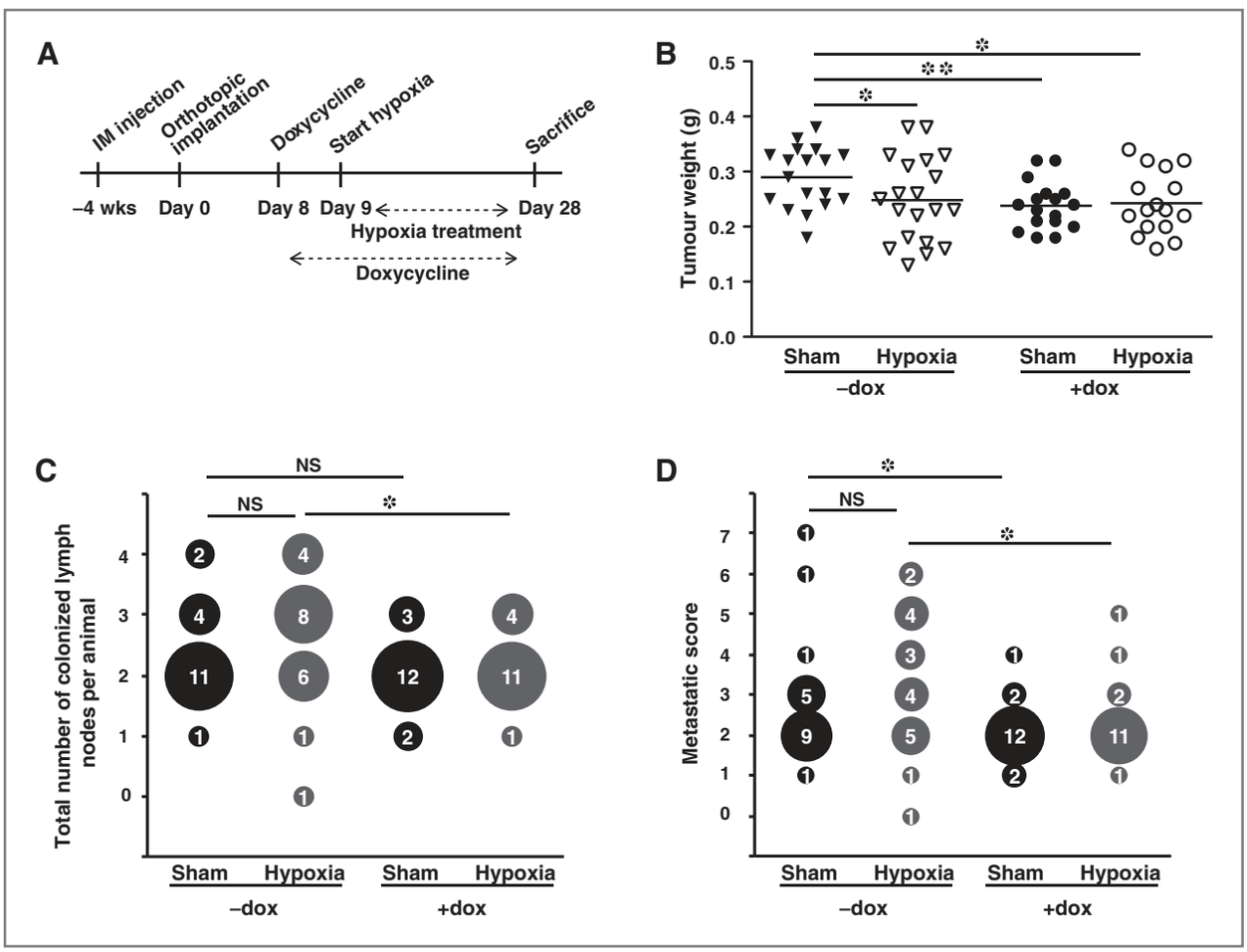

Figure 3. Inhibition of UPR signaling suppresses hypoxia-induced lymph node metastasis. A, timeline metastasis assay. Cervical tumors were initiated by orthotopic implantation of fragments derived from several different intramuscular ME180-GADD34-C tumors. B, size of orthotopic xenografts. The cervix tumors were excised and weighted at the end of the experiment (day 28). Each symbol represents a tumor from one animal. Horizontal lines represent the mean values for each group. Animals carrying tumors 2 SDs above or below group mean were excluded from analysis because of positive correlation between primary tumor size and lymph node metastasis (13). Unpaired Student *t* test, one-tailed; *, $P < 0.05$; **, $P < 0.005$. C, on the *y*-axis is shown the total number of colonized lymph nodes in each animal (of a total of 8). The size of the circle represents the number of animals (labeled in the center). D, on the *y*-axis is shown metastatic scores. The metastatic score for each animal was calculated using the formula: $(p_1 \times 1) + (p_2 \times 1) + (p_3 \times 2) + (p_4 \times 3)$ where p_1 is the number of involved nodes for lymph node pair 1, p_2 is the number of involved nodes for lymph node pair 2, etc. The size of the circle represents the number of animals (labeled in the center). Mann–Whitney test, one-tailed; *, $P < 0.05$.

Published OnlineFirst September 17, 2013; DOI: 10.1158/1078-0432.CCR-13-0526

PERK signaling also reduced primary tumor size (compare −dox and −dox sham) but only in the air-breathing group.

In agreement with previous publications, the control (doxycycline-free) group showed a trend toward increased numbers of lymph node metastases when exposed to hypoxia (Fig. 3C and Supplementary Fig. S5A; compare −dox sham and −dox hypoxia). In contrast, mice administered doxycycline to disrupt PERK signaling exhibited no evidence of increased metastasis when exposed to hypoxia (compare +dox sham and +dox hypoxia). The PERK signaling–deficient tumors produced similar numbers of metastases as controls under sham conditions but significantly less metastases than controls in the hypoxia-exposed group. Increased metastatic capacity in the ME180 orthotopic model is also reflected by colonization of more distal lymph nodes. To account for the location of involved nodes, we assigned weights to the 4 lymph node pairs based on their distance from the primary tumor and calculated a metastatic score for each animal. Similar to the effect on the total number of metastatic nodes, disruption of PERK signaling significantly decreased the metastatic score in hypoxia-treated animals (Fig. 3D and Supplementary Fig. S5B). Together, these results indicate that the PERK/eIF2α arm of the UPR promotes both primary tumor growth and hypoxia-induced nodal metastasis.

LAMP3 promotes hypoxia-induced lymph node metastasis

To directly assess the involvement of the PERK target gene LAMP3 in hypoxia-induced metastasis, we introduced stable expression of a short hairpin RNA targeting LAMP3 in ME180 cells and showed that it fully abrogated the hypoxia-induced increase in mRNA and protein (Supplementary Fig. S6A and S6B, respectively). Xenografts established from LAMP3-knockdown cells also showed a marked reduction in LAMP3 protein expression *in vivo* compared with controls (Fig. 4A and Supplementary Fig. S7).

Mice with orthotopic ME180 empty vector control and LAMP3-knockdown xenografts were exposed to the hypoxia regimen and assessed for primary tumor growth and metastasis to the pelvic lymph nodes. In contrast to disruption of PERK signaling (Fig. 3), knockdown of LAMP3 did not adversely affect tumor growth, and in fact both sham- and hypoxia-treated groups showed a trend toward somewhat larger primary tumors compared with their respective controls (Fig. 4B; compare EV and shLAMP3 sham). However, despite this trend to somewhat larger primary tumors, LAMP3 knockdown prevented hypoxia-induced metastasis to the lymph nodes. The EV control group showed a significant increase in metastasis under hypoxia as assessed by both total number of metastases (Fig. 4C and Supplementary Fig. S8A) and metastatic score (Fig. 4D and Supplementary Fig. S8B). In contrast, LAMP3-knockdown tumors showed no increase in the hypoxia treated group and in fact trended to have even fewer metastases than the sham-treated group. The results from this experiment suggest that hypoxia augments metastasis, in part, through the UPR-regulated gene LAMP3.

Activation of the PERK/eIF2α arm of the UPR promotes hypoxia tolerance

The potential mechanisms contributing to the defect in hypoxia-induced metastasis were investigated by characterizing the microenvironments of the orthotopic xenografts using IHC for vasculature, perfusion, and hypoxia. Although PERK signaling has been reported to regulate angiogenesis (21), we found no differences in vessel content or perfusion in the PERK signaling–deficient tumors exposed to sham treatment or to hypoxia (Fig. 5A and Supplementary Fig. S9). Several studies have also shown that activation of the PERK/eIF2α/ATF4 arm of the UPR increases hypoxia tolerance and consequently promotes higher levels of tumor hypoxia (20, 26, 40). The fact that the GADD34 tumors are smaller than controls is consistent with these observations (see Fig. 3B). To directly test the contribution of PERK signaling to hypoxia tolerance, we conducted clonogenic assays under hypoxia in dox-treated and untreated cells *in vitro*. Figure 5B shows that ME180-GADD34-C cells are indeed significantly more sensitive to anoxia-induced cell death following doxycycline. However, the large variation in the fraction of hypoxic tumor cells as assessed by EF5 staining *in vivo* makes it difficult to rule out a small contribution to overall hypoxia between tumors with intact versus inhibited PERK signaling (Fig. 5C and D). Nonetheless, although PERK signaling–deficient cells are more sensitive to hypoxia-induced cell death, differences in the proportion of viable hypoxic cells in the primary tumor cannot account alone for the loss of metastasis in the PERK signaling–deficient group.

LAMP3 influences migration of hypoxic cells

Characterization of the microenvironment of sham- and hypoxia-treated tumors also showed no difference in angiogenesis in the control versus LAMP3-knockdown tumors (Supplementary Fig. S10). LAMP3-deficient tumors did have a slightly larger hypoxic fraction compared to empty vector control tumors (Supplementary Fig. S11A), although this finding can be accounted for based on a strong relationship between primary tumor size and hypoxic fraction (Supplementary Fig. S11B). Unlike the PERK-deficient cells, LAMP3 knockdown and empty vector controls showed a comparable sensitivity to hypoxia-induced cell death in *in vitro* as assessed by clonogenic survival (Fig. 6A). These data suggest that LAMP3 does not promote hypoxia-induced metastasis through regulation of angiogenesis and/or hypoxia tolerance.

Although we found no direct role for LAMP3 on hypoxia tolerance, knockdown of LAMP3 did reduce colony formation in soft agar (Supplementary Fig. S12), an assay often used to assess anchorage-independent growth, a vital property of metastatic cells. We investigated a more direct role of LAMP3 in regulation of the metastatic phenotypes through a series of *in vitro* assays. First, we assessed migration under normoxic (21% O_2) and hypoxic (1% O_2) conditions in LAMP3 knockdown and empty vector control cells using *in vitro* Transwell migration assays. We found that LAMP3 knockdown resulted in a substantial loss in migration in this assay under hypoxic conditions (Fig. 6B). Knockdown of

Published OnlineFirst September 17, 2013; DOI: 10.1158/1078-0432.CCR-13-0526

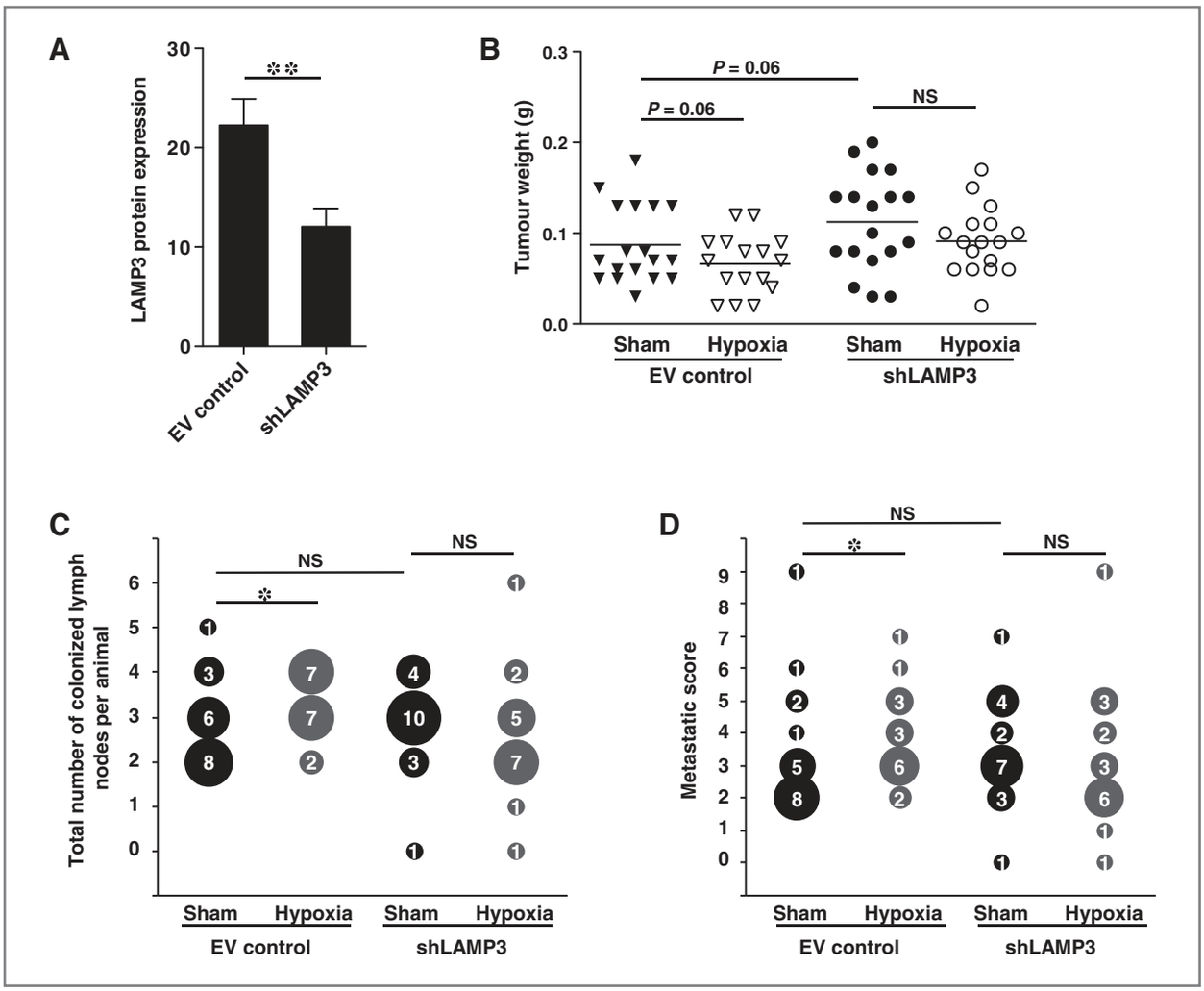

Figure 4. Knockdown of LAMP3 inhibits hypoxia-induced lymph node metastasis. A, quantification of LAMP3 protein expression as assessed by immunofluorescence staining in LAMP3 knockdown and empty vector control tumors. Bars represent the mean of 20 tumors. Error bars depict SEM. Unpaired Student *t* test, 2-tailed; **, $P < 0.005$. B, size of the orthotopic tumors at the end of the experiment, 25 days after orthotopic implantation. Each symbol represents a tumor from one animal. Horizontal lines represent the mean values for each group. Animals carrying tumors $\leq$0.01 g and/or 2 SDs above or below group mean were excluded from analysis. Unpaired Student *t* test, one-tailed. C, total number of colonized lymph nodes, see Fig. 3C. D, metastatic scores, see Fig. 3D. Mann–Whitney test, one-tailed; *, $P < 0.05$.

LAMP3 in the highly migratory HeLa cell line also resulted in a substantial reduction in Transwell migration that was similar in magnitude to that observed in ME180 cells, although results in this line showed more variability (Supplementary Fig. S13). Second, cell motility was also evaluated in ME180 cells using a 3-dimensional (3D) spheroid migration assay. Multicellular spheroid cultures grown in a 3D environment are characterized by a necrotic core surrounded by viable hypoxic cells and thus mimic some of the properties of cells grown *in vivo*. We observed that migration of cells out of the spheroids was strongly reduced by LAMP3 knockdown (Fig. 6C), reflecting impaired motility of the hypoxic LAMP3-deficient cells. Third, we measured cell migration in both ME180 and CaSki cell lines, which show similar migratory speeds, using the scratch wound-healing assay (Fig. 6D and Supplementary Fig. S14A and S14B respectively). We found that in both cases, loss of LAMP3 slowed cell migration in this assay, although the magnitude of effects was much smaller than in the Transwell and spheroid migration assays. We also used the wound-healing assay to determine whether overexpression of LAMP3 was sufficient to promote migration, even under aerobic conditions. Indeed, overexpression of LAMP3 moderately increased the rate of wound closure (Supplementary Fig. S14C and S14D). Taken together, these results are consistent with a model in which LAMP3 promotes metastasis during hypoxia by promoting cancer cell migration.

Discussion

Previous clinical studies have identified tumor hypoxia as an important predictor of metastasis in patients with cervical cancer treated with surgery and/or radiotherapy (5, 7).

Published OnlineFirst September 17, 2013; DOI: 10.1158/1078-0432.CCR-13-0526

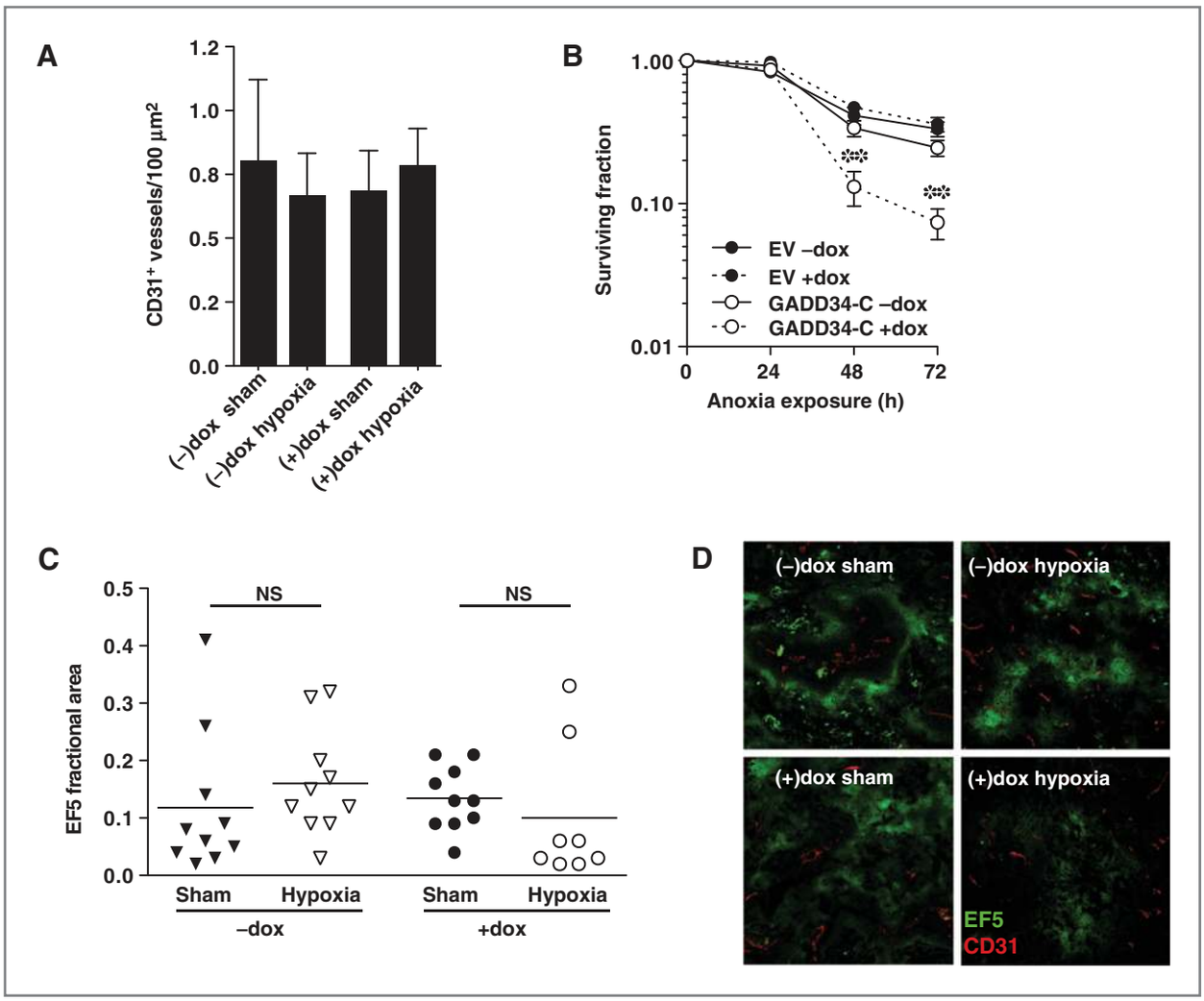

Figure 5. Activation of the PERK/eIF2α arm of the UPR promotes hypoxia tolerance. A, the microvessel density of ME180-GADD34-C orthotopic xenografts was evaluated by immunofluorescence staining (CD31). Bars represent the mean of 10 tumors. Error bars depict SD. B, clonogenic survival ME180-GADD34-C and empty vector control (EV) cells after exposure to anoxia in the presence or absence of doxycycline. Mean and SEM of 3 independent experiments is shown. One-way ANOVA; **, $P < 0.005$, (–)dox EV versus rest. C, fraction of EF5-labeled tumor area (left). Horizontal lines represent the mean values for each group. Unpaired Student *t* test, one-tailed; NS, not significant. D, dual immunofluorescence labeling for hypoxia (EF5, green) and vessels (CD31, red).

This includes previously published results from an ongoing study assessing hypoxia in patients with cervical cancer receiving radiotherapy at the Princess Margaret Cancer Centre (7). In this study of 106 patients, hypoxia was shown to be a significant prognostic marker for overall survival in a multivariate model, and this effect was due primarily to differences in distant metastasis rather than local control. Here, we used biopsies from the same trial involving a similar group of patients with cervical cancer. Our data show that in these patients, LAMP3 expression is regulated by both genetic gains/amplifications of LAMP3 and tumor hypoxia. Similar to other studies in cervix cancer (38), approximately 40% of all patients showed copy number aberrations and this was associated with increased LAMP3 mRNA and protein expression. However, in the other 60% with no copy number aberrations, we found that hypoxia was strongly and significantly associated with LAMP3 expression. We did not find a statistically significant association of LAMP3 with poor outcome in these patients, but this is likely influenced by the low statistical power of the study (hypoxic status also did not reach significance in this small cohort). However, the fact that LAMP3 is significantly associated with hypoxia, which has been shown to drive poor outcome in larger patient cohorts, strongly implicates LAMP3 as a contributor to metastasis in these patients.

Our *in vivo* data support a role for the PERK/eIF2α/ATF4 arm of the UPR and LAMP3 in particular in hypoxia-driven metastasis. We have presented evidence for 2 different contributions of this pathway to hypoxia-induced metastasis. The first is through a direct influence on the tolerance

Published OnlineFirst September 17, 2013; DOI: 10.1158/1078-0432.CCR-13-0526

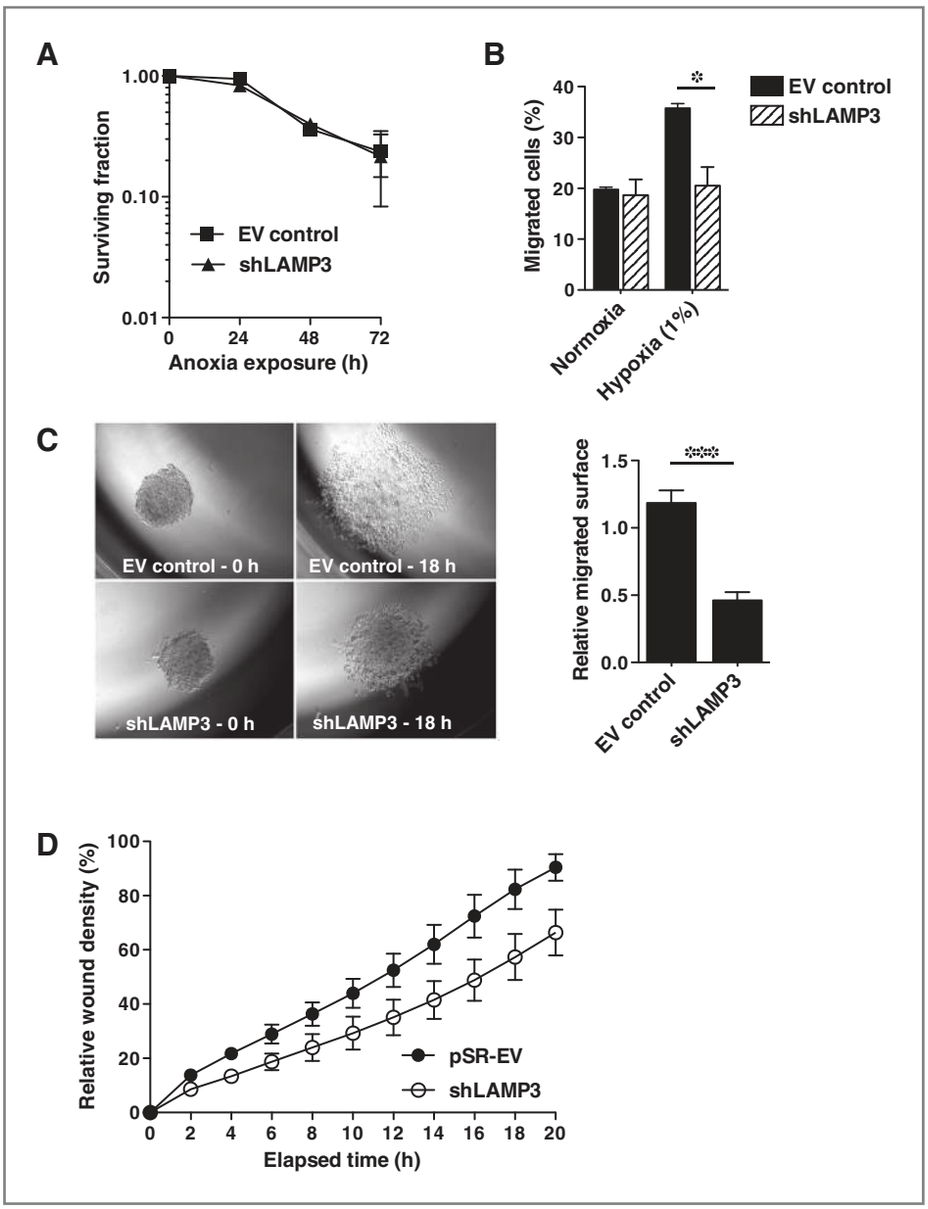

Figure 6. LAMP3 promotes cell migration and invasion during hypoxia. A, clonogenic survival shLAMP3 and empty vector control cells in response to anoxic exposure. Mean and SEM of 3 independent experiments are shown. B, Transwell migration assay. Migration of shLAMP3 and empty vector control cells was monitored during both normoxic and hypoxic (1% oxygen) conditions. Mean and SEM of 2 independent experiments are shown. Two-way ANOVA; *, $P < 0.05$. C, 3-dimensional spheroid migration assay. Left, representative images of shLAMP3 and empty vector control spheroids. Right, area covered by migrating cells during a period of 18 hours. Mean and SEM of all wells from 2 independent experiments are shown. Unpaired Student *t* test; ***, $P < 0.0001$. D, scratch wound-healing assay. Closure of the scratch wound by ME180 LAMP3-knockdown and empty vector control cells. Relative wound density is a measure of the density of the wound region relative to the density of the cell region and is expressed in percentages. Mean and SEM of 2 independent experiments are shown.

of cells to hypoxia, as overexpression of GADD34 markedly reduced cell survival in cells exposed to hypoxia *in vitro* and also impaired tumor growth *in vivo*. These data are consistent with other reports showing that the UPR pathway is an important mediator of hypoxia tolerance and tumor growth by affecting cellular processes that include autophagy, angiogenesis, and pH regulation (19–21, 26, 41). Tumor cells with a higher hypoxia tolerance, by definition, have a higher probability to escape the primary tumor and survive in an avascular metastatic site regardless of how or when they acquire other metastatic phenotypes. However, tolerance mechanisms cannot alone account for the PERK contribution to hypoxia-induced metastasis in our model. We did not observe significant differences in overall levels of hypoxia in the PERK signaling proficient and deficient tumors at the end of the hypoxia treatment schedule. Instead, our data suggest that PERK/eIF2α regulation of LAMP3 is a key driver of both the migratory phenotype and development of lymph node metastases in response to hypoxia. Silencing LAMP3 caused no reduction in hypoxia tolerance *in vitro*, hypoxic fraction *in vivo*, or primary tumor size but did effectively inhibit hypoxia-induced metastasis *in vivo* and hypoxia-induced migration in 3 different *in vitro* models. Interestingly, knockdown of VEGF-C signaling also achieves a reduction in hypoxia-induced metastasis in this model (36). Thus, it is clear that multiple pathways are likely contributing and required to observe increased metastasis in response to hypoxia

LAMP3 and its functional role in cancer have not been investigated in much detail. LAMP3 and other LAMP family

Published OnlineFirst September 17, 2013; DOI: 10.1158/1078-0432.CCR-13-0526

members are lysosomal membrane glycoproteins characterized by a long luminal domain containing multiple O- and N-linked glycosylation sites as well as several disulfide bonds, a transmembrane domain, and a short cytoplasmic tail (42). Cell surface expression of LAMPs is often observed in cancer cells and has been shown to correlate with the metastatic ability of colon carcinoma cell lines (43). We identified LAMP3 as a hypoxia-responsive gene regulated by PERK/eIF2α signaling and showed that it is also found on the cell surface (33). We also showed that LAMP3 is overexpressed in breast cancer (33) and moreover that it is an independent prognostic factor for locoregional control in a subgroup of patients treated with radiotherapy (44). However, the biologic function of LAMP3 in migration and metastasis in tumor cells is not understood. LAMP1 was shown to be required for proper formation of membrane ruffles and filopodia in migrating tumor cells (45) and it is possible that LAMP3 exerts a similar function in response to hypoxia. A role for LAMP3 in cell–cell adhesion has also been proposed as it is a highly glycosylated protein that is often localized to the cell surface of tumor cells (42, 46), and other LAMP family members have already been implicated in cell adhesion (47). By mediating binding to endothelial cells for example, LAMP3 might facilitate tumor cell extravasation.

These data support accumulating evidence implicating ER stress responses as important contributors to aggressive hypoxic tumor biology (19, 26, 41). This potential importance of ER stress responses in cancer has led to some attempts to identify and incorporate agents aimed at disrupting ER homeostasis either alone or in combination with conventional agents (26, 48–50). Our findings suggest that such agents are likely to be most effective when given in curative settings in combination with conventional therapy or with other agents that target well-oxygenated cells. This approach would produce synergy not only by targeting distinct populations of cells in the tumor but also by targeting intrinsic mechanisms that enable the hypoxic cells to escape and colonize distant nodes or other organs.

Disclosure of Potential Conflicts of Interest

The views expressed do not necessarily reflect those of the OMOHLT. B.G. Wouters has a Commercial Research Grant from Pfizer. No potential conflicts of interest were disclosed.

Authors' Contributions

Conception and design: H. Mujcic, M. Milosevic, M. Koritzinsky, B.G. Wouters

Development of methodology: H. Mujcic, S. Chung, N. Chaudary, R.P. Hill, B.G. Wouters

Acquisition of data (provided animals, acquired and managed patients, provided facilities, etc.): H. Mujcic, A. Nagelkerke, K.M.A. Rouschop, S. Chung, N. Chaudary, P.N. Span, B. Clarke, M. Milosevic

Analysis and interpretation of data (e.g., statistical analysis, biostatistics, computational analysis): H. Mujcic, K.M.A. Rouschop, M. Milosevic, J. Sykes, M. Koritzinsky, B.G. Wouters

Writing, review, and/or revision of the manuscript: H. Mujcic, A. Nagelkerke, K.M.A. Rouschop, N. Chaudary, P.N. Span, B. Clarke, M. Milosevic, J. Sykes, M. Koritzinsky, B.G. Wouters

Administrative, technical, or material support (i.e., reporting or organizing data, constructing databases): H. Mujcic, B.G. Wouters

Study supervision: K.M.A. Rouschop, R.P. Hill, M. Koritzinsky, B.G. Wouters

Acknowledgments

The authors thank Anthony Fyles for providing uterine cervix cancer TMA sections and Trevor Do, Trudey Nicklee, and Melanie Macasaet for advice and technical assistance on the immunohistochemical stainings in these and other tissue samples. They also thank Olga Ludkovski for the FISH analysis, Melania Pintilie for help with the statistical analysis, and Ravi Vellanki for his assistance with confocal microscopy.

Grant Support

This work was financially supported by the Ontario Ministry of Health and Long Term Care (OMOHLTC), the Terry Fox New Frontiers Research Program (PPG09-020005 to B.G. Wouters and M. Koritzinsky), the Ontario Institute for Cancer Research and Terry Fox Research Institute (Selective therapies program to B.G. Wouters), the Canadian Institute for Health Research (CIHR grant 201592 to B.G. Wouters and M. Koritzinsky and CIHR grant 102757 to R.P. Hill), the Dutch Cancer Society (KWF grant UM 2008-4068 to B.G. Wouters), the transnationale Universiteit Limburg (TUL 30943099T to B.G. Wouters), the EU 7th framework program (METOXIA project 222741 to B.G. Wouters and M. Koritzinsky), and the Terry Fox New Investigator awarded to M. Koritzinsky.

The costs of publication of this article were defrayed in part by the payment of page charges. This article must therefore be hereby marked *advertisement* in accordance with 18 U.S.C. Section 1734 solely to indicate this fact.

Received February 26, 2013; revised August 23, 2013; accepted September 12, 2013; published OnlineFirst September 17, 2013.

References

1. Brizel DM, Sibley GS, Prosnitz LR, Scher RL, Dewhirst MW. Tumor hypoxia adversely affects the prognosis of carcinoma of the head and neck. Int J Radiat Oncol Biol Phys 1997;38:285–9.
2. Hockel M, Knoop C, Schlenger K, Vorndran B, Baussmann E, Mitze M, et al. Intratumoral pO2 predicts survival in advanced cancer of the uterine cervix. Radiother Oncol 1993;26:45–50.
3. Nordsmark M, Overgaard J. A confirmatory prognostic study on oxygenation status and loco-regional control in advanced head and neck squamous cell carcinoma treated by radiation therapy. Radiother Oncol 2000;57:39–43.
4. Brizel DM, Scully SP, Harrelson JM, Layfield LJ, Bean JM, Prosnitz LR, et al. Tumor oxygenation predicts for the likelihood of distant metastases in human soft tissue sarcoma. Cancer Res 1996;56:941–3.
5. Hockel M, Schlenger K, Aral B, Mitze M, Schaffer U, Vaupel P. Association between tumor hypoxia and malignant progression in advanced cancer of the uterine cervix. Cancer Res 1996;56:4509–15.
6. Pitson G, Fyles A, Milosevic M, Wylie J, Pintilie M, Hill R. Tumor size and oxygenation are independent predictors of nodal diseases in patients with cervix cancer. Int J Radiat Oncol Biol Phys 2001;51:699–703.
7. Fyles A, Milosevic M, Hedley D, Pintilie M, Levin W, Manchul L, et al. Tumor hypoxia has independent predictor impact only in patients with node-negative cervix cancer. J Clin Oncol 2002;20:680–7.
8. Milosevic M, Warde P, Menard C, Chung P, Toi A, Ishkanian A, et al. Tumor hypoxia predicts biochemical failure following radiotherapy for clinically localized prostate cancer. Clin Cancer Res 2012;18:2108–14.
9. Rofstad EK, Danielsen T. Hypoxia-induced metastasis of human melanoma cells: involvement of vascular endothelial growth factor-mediated angiogenesis. Br J Cancer 1999;80:1697–707.
10. Stackpole CW, Groszek L, Kalbag SS. Benign-to-malignant B16 melanoma progression induced in two stages in vitro by exposure to hypoxia. J Natl Cancer Inst 1994;86:361–7.
11. Young SD, Hill RP. Effects of reoxygenation on cells from hypoxic regions of solid tumors: anticancer drug sensitivity and metastatic potential. J Natl Cancer Inst 1990;82:371–80.
12. Young SD, Marshall RS, Hill RP. Hypoxia induces DNA overreplication and enhances metastatic potential of murine tumor cells. Proc Natl Acad Sci U S A 1988;85:9533–7.

Published OnlineFirst September 17, 2013; DOI: 10.1158/1078-0432.CCR-13-0526

13. Cairns RA, Hill RP. Acute hypoxia enhances spontaneous lymph node metastasis in an orthotopic murine model of human cervical carcinoma. Cancer Res 2004;64:2054–61.
14. Cairns RA, Kalliomaki T, Hill RP. Acute (cyclic) hypoxia enhances spontaneous metastasis of KHT murine tumors. Cancer Res 2001; 61:8903–8.
15. Rofstad EK, Gaustad JV, Egeland TA, Mathiesen B, Galappathi K. Tumors exposed to acute cyclic hypoxic stress show enhanced angiogenesis, perfusion and metastatic dissemination. Int J Cancer 2010;127:1535–46.
16. Harris AL. Hypoxia–a key regulatory factor in tumour growth. Nat Rev Cancer 2002;2:38–47.
17. Blais JD, Filipenko V, Bi M, Harding HP, Ron D, Koumenis C, et al. Activating transcription factor 4 is translationally regulated by hypoxic stress. Mol Cell Biol 2004;24:7469–82.
18. Koumenis C, Naczki C, Koritzinsky M, Rastani S, Diehl A, Sonenberg N, et al. Regulation of protein synthesis by hypoxia via activation of the endoplasmic reticulum kinase PERK and phosphorylation of the translation initiation factor eIF2alpha. Mol Cell Biol 2002;22:7405–16.
19. Romero-Ramirez L, Cao H, Nelson D, Hammond E, Lee AH, Yoshida H, et al. XBP1 is essential for survival under hypoxic conditions and is required for tumor growth. Cancer Res 2004;64:5943–7.
20. Bi M, Naczki C, Koritzinsky M, Fels D, Blais J, Hu N, et al. ER stress-regulated translation increases tolerance to extreme hypoxia and promotes tumor growth. EMBO J 2005;24:3470–81.
21. Blais JD, Addison CL, Edge R, Falls T, Zhao H, Wary K, et al. Perk-dependent translational regulation promotes tumor cell adaptation and angiogenesis in response to hypoxic stress. Mol Cell Biol 2006;26: 9517–32.
22. Koritzinsky M, Rouschop KM, van den Beucken T, Magagnin MG, Savelkouls K, Lambin P, et al. Phosphorylation of eIF2alpha is required for mRNA translation inhibition and survival during moderate hypoxia. Radiother Oncol 2007;83:353–61.
23. Ameri K, Lewis CE, Raida M, Sowter H, Hai T, Harris AL. Anoxic induction of ATF-4 through HIF-1-independent pathways of protein stabilization in human cancer cells. Blood 2004;103:1876–82.
24. Harding HP, Novoa I, Zhang Y, Zeng H, Wek R, Schapira M, et al. Regulated translation initiation controls stress-induced gene expression in mammalian cells. Mol Cell 2000;6:1099–108.
25. Harding HP, Zhang Y, Zeng H, Novoa I, Lu PD, Calfon M, et al. An integrated stress response regulates amino acid metabolism and resistance to oxidative stress. Mol Cell 2003;11:619–33.
26. Rouschop KM, van den Beucken T, Dubois L, Niessen H, Bussink J, Savelkouls K, et al. The unfolded protein response protects human tumor cells during hypoxia through regulation of the autophagy genes MAP1LC3B and ATG5. J Clin Invest 2010;120:127–41.
27. Ma Y, Hendershot LM. Delineation of a negative feedback regulatory loop that controls protein translation during endoplasmic reticulum stress. J Biol Chem 2003;278:34864–73.
28. Chan DA, Giaccia AJ. Hypoxia, gene expression, and metastasis. Cancer Metastasis Rev 2007;26:333–9.
29. Lunt SJ, Chaudary N, Hill RP. The tumor microenvironment and metastatic disease. Clin Exp Metastasis 2009;26:19–34.
30. Erler JT, Bennewith KL, Cox TR, Lang G, Bird D, Koong A, et al. Hypoxia-induced lysyl oxidase is a critical mediator of bone marrow cell recruitment to form the premetastatic niche. Cancer Cell 2009; 15:35–44.
31. Yang MH, Wu MZ, Chiou SH, Chen PM, Chang SY, Liu CJ, et al. Direct regulation of TWIST by HIF-1alpha promotes metastasis. Nat Cell Biol 2008;10:295–305.
32. Osinsky SP, Ganusevich II, Bubnovskaya LN, Valkovskaya NV, Kovelskaya AV, Sergienko TK, et al. Hypoxia level and matrix metalloproteinases-2 and -9 activity in Lewis lung carcinoma: correlation with metastasis. Exp Oncol 2005;27:202–5.
33. Mujcic H, Rzymski T, Rouschop KM, Koritzinsky M, Milani M, Harris AL, et al. Hypoxic activation of the unfolded protein response (UPR) induces expression of the metastasis-associated gene LAMP3. Radiother Oncol 2009;92:450–9.
34. Kanao H, Enomoto T, Kimura T, Fujita M, Nakashima R, Ueda Y, et al. Overexpression of LAMP3/TSC403/DC-LAMP promotes metastasis in uterine cervical cancer. Cancer Res 2005;65:8640–5.
35. Novoa I, Zeng H, Harding HP, Ron D. Feedback inhibition of the unfolded protein response by GADD34-mediated dephosphorylation of eIF2alpha. J Cell Biol 2001;153:1011–22.
36. Chaudary N, Milosevic M, Hill RP. Suppression of vascular endothelial growth factor receptor 3 (VEGFR3) and vascular endothelial growth factor C (VEGFC) inhibits hypoxia-induced lymph node metastases in cervix cancer. Gynecol Oncol 2011;123:393–400.
37. Fyles A, Milosevic M, Pintilie M, Syed A, Levin W, Manchul L, et al. Long-term performance of interstial fluid pressure and hypoxia as prognostic factors in cervix cancer. Radiother Oncol 2006;80: 132–7.
38. Wangsa D, Heselmeyer-Haddad K, Ried P, Eriksson E, Schaffer AA, Morrison LE, et al. Fluorescence in situ hybridization markers for prediction of cervical lymph node metastases. Am J Pathol 2009; 175:2637–45.
39. Cairns RA, Hill RP. A fluorescent orthotopic model of metastatic cervical carcinoma. Clin Exp Metastasis 2004;21:275–81.
40. Rouschop KM, Dubois L, Keulers T, van den Beucken T, Lambin P, Bussink J, et al. PERK/eIF2α signaling protects therapy resistant hypoxic cells through induction of glutathione synthesis and protection against ROS. Proc Natl Acad Sci U S A 2013;110: 4622–7.
41. van den Beucken T, Ramaekers CH, Rouschop K, Koritzinsky M, Wouters BG. Deficient carbonic anhydrase 9 expression in UPR-impaired cells is associated with reduced survival in an acidic microenvironment. Radiother Oncol 2009;92:437–42.
42. de Saint-Vis B, Vincent J, Vandenabeele S, Vanbervliet B, Pin JJ, Ait-Yahia S, et al. A novel lysosome-associated membrane glycoprotein, DC-LAMP, induced upon DC maturation, is transiently expressed in MHC class II compartment. Immunity 1998;9:325–36.
43. Saitoh O, Wang WC, Lotan R, Fukuda M. Differential glycosylation and cell surface expression of lysosomal membrane glycoproteins in sublines of a human colon cancer exhibiting distinct metastatic potentials. J Biol Chem 1992;267:5700–11.
44. Nagelkerke A, Mujcic H, Bussink J, Wouters BG, van Laarhoven HW, Sweep FC, et al. Hypoxic regulation and prognostic value of LAMP3 expression in breast cancer. Cancer 2011;117:3670–81.
45. Garrigues J, Anderson J, Hellstrom KE, Hellstrom I. Anti-tumor antibody BR96 blocks cell migration and binds to a lysosomal membrane glycoprotein on cell surface microspikes and ruffled membranes. J Cell Biol 1994;125:129–42.
46. Ozaki K, Nagata M, Suzuki M, Fujiwara T, Ueda K, Miyoshi Y, et al. Isolation and characterization of a novel human lung-specific gene homologous to lysosomal membrane glycoproteins 1 and 2: significantly increased expression in cancers of various tissues. Cancer Res 1998;58:3499–503.
47. Sawada R, Lowe JB, Fukuda M. E-selectin-dependent adhesion efficiency of colonic carcinoma cells is increased by genetic manipulation of their cell surface lysosomal membrane glycoprotein-1 expression levels. J Biol Chem 1993;268:12675–81.
48. Feldman D. Irestatin, a potent inhibitor of IRE1α and the unfolded protein response, is a hypoxia-selective cytotoxin and impairs tumor growth. ASCO Annual Meeting Proceedings 25;18S (June 20 Supplement), 2007. Abstract nr 3514.
49. Davenport EL, Moore HE, Dunlop AS, Sharp SY, Workman P, Morgan GJ, et al. Heat shock protein inhibition is associated with activation of the unfolded protein response pathway in myeloma plasma cells. Blood 2007;110:2641–9.
50. Obeng EA, Carlson LM, Gutman DM, Harrington WJ Jr, Lee KP, Boise LH. Proteasome inhibitors induce a terminal unfolded protein response in multiple myeloma cells. Blood 2006;107:4907–16.